CHAPTER 118

IMPACT LOADS INDUCED BY PLUNGING BREAKERS ON VERTICAL STRUCTURES

Schmidt, R.[1] ; Oumeraci, H.[2] ; Partenscky, H.-W.[3]

Abstract

Results of large-scale model tests on impact loading of a vertical wall by using waves up to 2 m height and 9.4 s period are presented. A classification of the breaker types tested and breaking criteria for waves in front of a vertical wall are suggested. Impact pressure distributions, forces and force impulses induced by plunging breakers on a vertical wall are discussed. The statistical distributions of the impact pressures and forces for different breaker types are also given. Some aspects of the generation mechanisms of impact pressures and the role of air content and its statistical distribution in the impact process are outlined.

Introduction

It has often been suggested in the literature that impact pressure induced by breaking waves has no structural significance, and hence should not be used for design purposes. One of the main reasons for this view point may certainly be explained by the static approach yet used to study the stability of vertical structures. The results of a study on vertical breakwater failures (OUMERACI et.al., 1991) together with the results of more recent investigations on the effect of impact loads on a vertical breakwater (OUMERACI et.al., 1992; TAKAHASHI et.al., 1992) have shown that impact pressure has not only a very localized effect, but may also be detrimental for the stability of the structure components as well as for the overall stability of the structure, including the foundation; i.e. the stability

---

[1] Dipl.-Ing., Research Engineer, GROSSER WELLENKANAL (GWK)

[2] Dr.-Ing., Senior Research Engineer, Sonderforschungsbereich 205

[3] Prof. Dr.-Ing. Dr.-Phys., Formerly Managing Director Franzius-Institut

of monolithic structures subject to breaking waves is of purely dynamic nature and cannot be simply reduced to a static problem.

For the dynamic stability analysis, detailed spatial and temporal pressure distributions with the corresponding force histories are required. However, reliable laboratory measurements in the impact area generally represent a very difficult task due to the highly transient and complex nature of the two-phase flow and pressure field involved, as well as to the scale effects related to air entrainment/entrapment. Therefore, a detailed large-scale model study on impact pressures due to breaking waves on a vertical wall has recently been performed in the Large Wave Flume (GWK) of Hannover. It is the main purpose of the paper to discuss some of the results of this study.

Experimental Set-Up and Test Conditions

The hydraulic model tests were performed in the Large Wave Flume of Hannover (320×5×7 m) by using regular and irregular waves up to 2 m height and 9.4 s period. The experimental set-up is given in Fig. 1, showing a) a sloping seabed 1:20 terminated by a vertical stiff wall of 6 m height instrumented with 28 high resolution pressure transducers ($f_N > 35$ kHz), and b) the locations of eleven wave gauges installed in front of the wall.
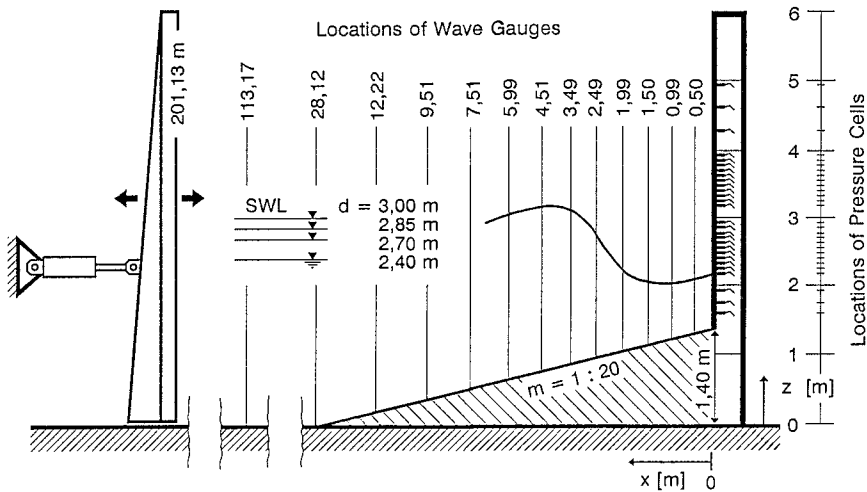

Fig. 1. Experimental Set-Up in the Large Wave Flume (GWK)

Water depths in the flume up to 3.0 m (1.6 m at the wall) were used for the tests. Most of the waves used in the tests arrive at the wall as plunging breakers, the maximum breaker heights obtained are in the range of $H_b = 1.15 \cdot d_b$, where d_b is the breaking depth measured from SWL.

Breaker Types and Kinematics

Breaker Types

A strong correlation exists between the shapes of the breaking waves at the vertical wall and the trapped air. On the other hand, the latter is known to considerably affect the magnitude as well as the spatial and temporal distribution of the impact pressure. Therefore, an attempt was first made to classify the breaker types obtained for the conditions tested, before any further analysis of the results was undertaken. In fact, different breaking wave conditions in comparison to those on an unobstructed beach are expected (GALVIN, 1968). For this purpose, video records as well as wave profiles obtained from wave gauge measurements were used. Depending on the value of H_b/d_w and on further parameters, seven types of breaking and broken waves — five for the plunging and two for the spilling breaker — in front of the vertical wall were obtained (Fig. 2). The water depth d_w directly at the vertical wall corresponds to the breaking depth d_b measured from SWL by the linear relationship $d_w = 0.80 \cdot d_b$ (average from 705 breaking waves and correlation coeff. of 0.84).
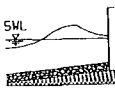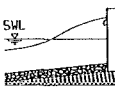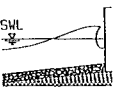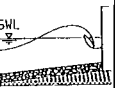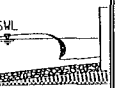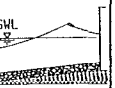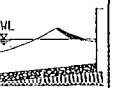
| Plunging breaker					Spilling breaker	
upward deflected	well developed		broken		well developed	broken
$\dfrac{H_b}{d_w}=0{,}92$	$\dfrac{H_b}{d_w}=0{,}99$	$\dfrac{H_b}{d_w}=1{,}06$	$\dfrac{H_b}{d_w}=1{,}14$		$\dfrac{H_b}{d_w}=0{,}99$	$\dfrac{H_b}{d_w}=1{,}14$
Type 1	Type 2	Type 3	Type 4	Type 5	Type 6	Type 7

Fig. 2.   Breaker Types Observed during Tests in GWK

In the following, however, special emphasis was put on the analysis of the results related to plunging breakers.

Breaking Criteria

Existing formulae for the prediction of the maximum breaker height H_b (or of the breaking depth d_b) as a function of the wave period T and the beach slope m (see for instance Eq. (2.92) in C.E.R.C., 1984) are related to waves on an unobstructed beach slope. Due to a full obstruction by a vertical wall in the flume, waves with $H_o/L_o = 0.0075 - 0.013$ were found to break in a depth d_b which is about 30 % higher than those predicted by the C.E.R.C. - formula. This is shown for instance by Fig. 3 in which the results of WEGGEL (1968) have also been plotted for comparison.
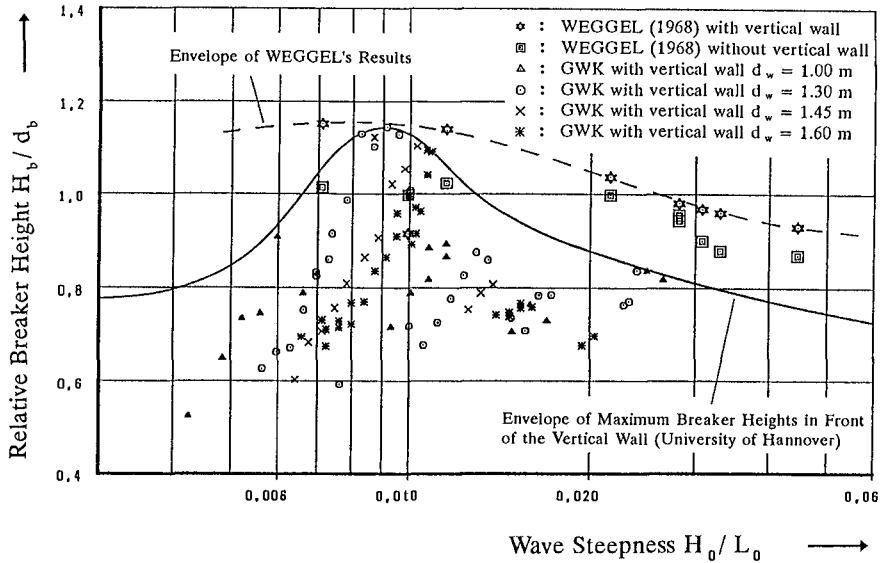
Fig. 3.   Maximum Breaker Heights in Front of a Vertical Wall

It is seen that in the presence of a vertical wall, a maximum breaker height H_b may occur which is almost 20 % larger than the breaking depth d_b. The corresponding deep water wave steepness is about 0.009.

Velocity and Volume of Wave at Breaking

The wave profiles in front of the vertical wall recorded by the wave gauges and video are shown for different time steps in Fig. 4. The
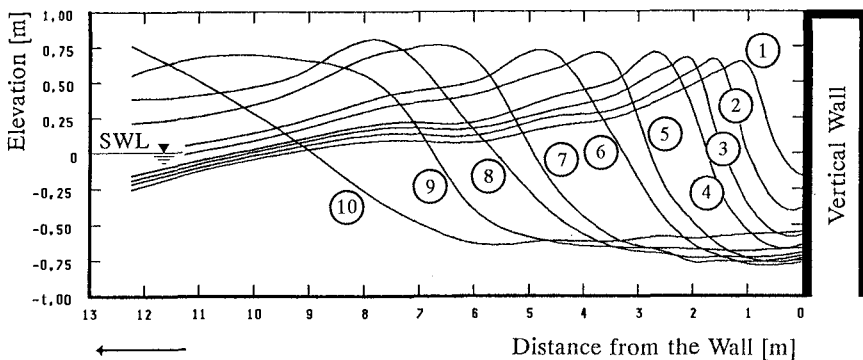

Fig. 4.   Wave Profiles in Front of a Vertical Wall at Different Time Steps

velocities and the volume of the wave at the instant of breaking are determined from such wave profile developments like those in Fig. 4 and compared to those predicted by different wave theories (linear wave theory, modified linear wave theory by GODA (1964) and solitary wave theory). It was found that for both the velocities u_s and the volume of the wave V_s at breaking, the solitary wave theory provides the best approximation:

$$u_s = \sqrt{g \cdot (d_b + H_b)} \qquad (1) \qquad\qquad V_s = \sqrt{\frac{16}{3} \cdot H_b \cdot d_b{}^3} \qquad (2)$$

where d_b is the breaking depth measured from SWL and H_b the breaker height, respectively. This is an important result as the momentum tranferred by a breaking wave to the wall may be approximately evaluated directly by using Eqs. (1) and (2). A comparison of such an approximation with the related force impulse obtained from pressure measurements will be shown later in Fig. 10.

Impact Loads

Influence of Sampling Frequency on measured Impact Loads

The first step when measured highly dynamic processes generally consists in evaluating the proper sampling rate. Therefore, the effect of the sampling frequency Δf on the peak pressures, peak forces and impulses has been investigated for $\Delta f = 0.1 - 11$ kHz. The results obtained show particulary that:

a) For the <u>pressure peaks</u>, sampling rates of $\Delta f = 2$, 1 and 0.175 kHz result in a reduction of 2, 7 and 50 %, respectively;

b) For the <u>force peaks</u>, sampling rates of $\Delta f = 2$, 1, 0.175 and 0.1 kHz result in a reduction of 2, 3, 20 and 37 %, respectively;

c) For the <u>force impulses,</u> no significant changes results even if the sampling rate is reduced to 0.1 kHz.

Impact Pressures and Forces

For each of the breaker types in Fig. 2, the following results can be obtained:

a) Simultaneous pressure histories at the 28 wall elevations by using a sampling frequency of 11 kHz;

b) Pressure distributions along the wall for time steps $\Delta t = 0.09 - 10$ ms.

For instance, some pressure distributions arc given in Fig. 5 (breaker height $H_b = 1.57$ m and wave period $T = 6.75$ s) at eleven different time steps. The horizontal force F_h per linear meter obtained from pressure integration is also given. Fig. 5 also illustrates that impact pressures are not only limited to small local areas but may also occur simultaneously over a large height (in a range up to the wave height!) of the vertical wall.

Particularly in the case of well-developed plunging breakers with large entrapped air pocket, the spatial integration of the impact pressures generally leads to a total force with a duration which may be much larger than usually assumed. In fact, the duration of total impact forces may reach 5 to 10 times that of the corresponding impact pressures. Since the latter is generally in the range of $0.05 - 0.02\,\text{s}$ (in the model), the duration of the total impact force may reach values in the range of $0.05 - 0.2\,\text{s}$ corresponding to values of $0.15 - 0.6\,\text{s}$ in prototype; i.e. values which may be in the same range or higher as the natural period of oscillations of common prototype caisson breakwaters: $T_N = 0.2 - 0.4\,\text{s}$ (MURAKI, 1966).
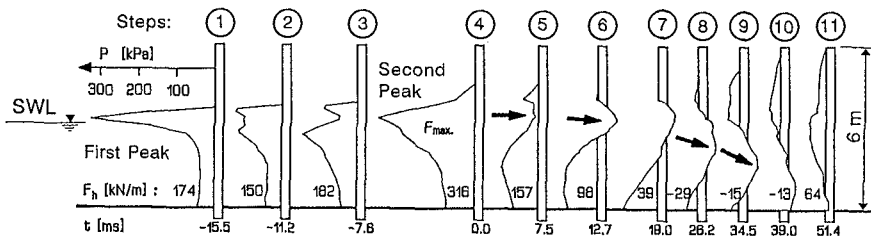

Fig. 5. Pressure Distributions at Different Time Steps (H_b=1.57 m ; T=6.75 s)

The origin of negative pressure (see Fig. 5, steps $6-10$) can also be explained by the fact that the trapped air is compressed so much that in re-expanding it throws the water mass back with such a velocity that the pressure drops below the atmospheric pressure value. The pressure distributions in Fig. 5 clearly characterize the impact of a plunging breaker with a large air pocket entrapped between the breaker front and the wall.
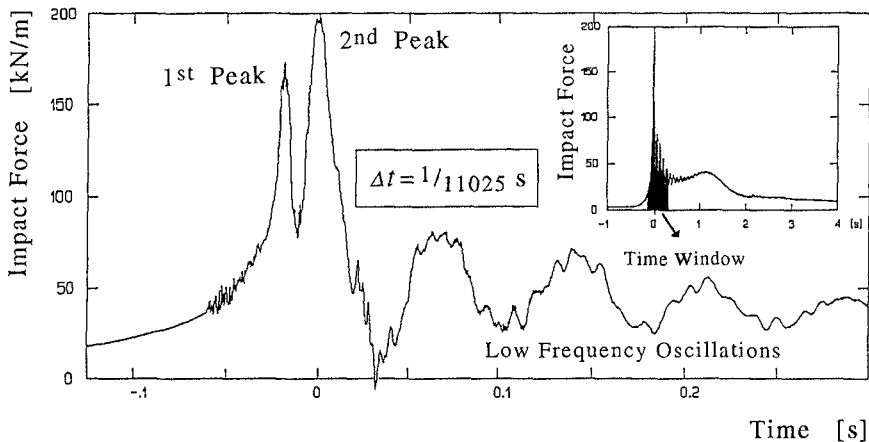

Fig. 6. Horizontal Force History Resulting from Pressure Integration

Typically, two force peaks (time step 1 + 4) occur which are also seen in the related force history shown in Fig. 6. A further important characteristic of this type of impact (well-developed plunging breaker with entrapped large air pocket) is the presence of the relative low frequency oscillations after the force peak (see Fig. 6). The latter are caused by the cyclic compressions and expansions of the entrapped air pocket under the highly transient pressure fields, and are hence related to the size of the entrapped air pocket. The equivalent diameter D_0 of the air pocket at its initial stage can be determined from the period T_{osc} of the force oscillations by the following relationship (OUMERACI et.al., 1992): $D_0 = k_a \cdot T_{osc}$ where $k_a = 5.35$ m/s. This means that the force oscillations with $T_{osc} = 0.075$ s in Fig. 6 corresponds to a trapped air pocket of $D_0 = 0.40$ m in the large-scale model. The period of the force oscillations transferred to prototype conditions may also lie in the range of the natural period of prototype caisson breakwaters: $T_N = 0.2 - 0.4$ s (MURAKI, 1966). These force oscillations may lead to near resonance excitation.
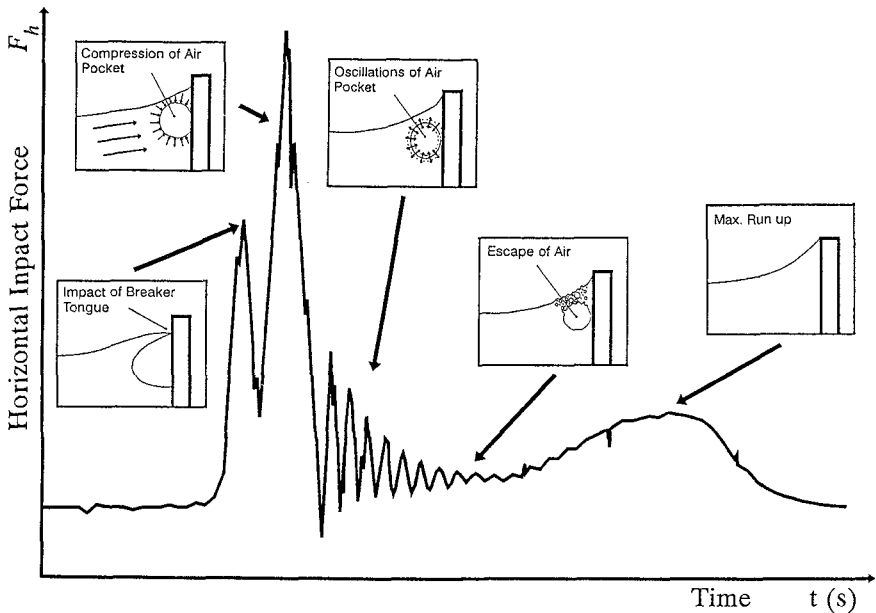

Fig. 7. Characteristics of Impact Forces and their Origin

The typical features of a force history caused by the impact of a breaker plunging on a vertical wall and entrapping a large air pocket are schematically summarized in Fig. 7 which also illustrates the origin of each of these characteristics.
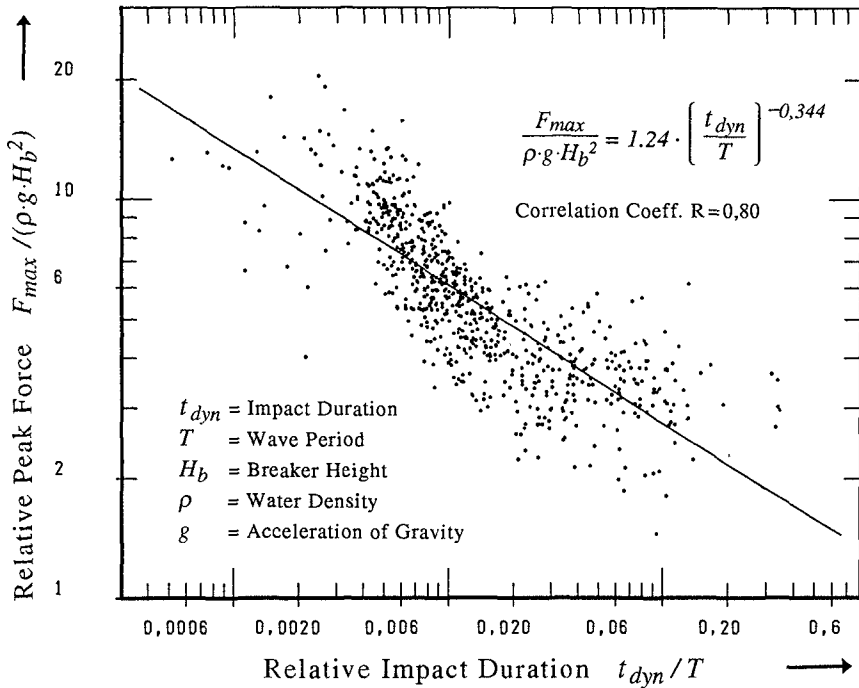
Fig. 8.   Duration of Impact Force

Duration of Impact Forces

Since the duration of the total impact force t_{dyn} constitutes an important characteristic of the dynamic loading, a relationship between t_{dyn} (related to wave period T) and the dimensionless maximum peak force F_{max} (related to the squared breaker height H_b) has been determined in Fig. 8, showing that t_{dyn} is almost inversely proportional to F^2_{max}. The extreme values of F_{max} generally occur for a deep water wave steepness $H_o/L_o \approx 0.005$. For lower or larger values of H_o/L_o, F_{max} decreases abruptly. For the force impulse, however, the extreme values occurs for $H_o/L_o \approx 0.0075$.

Force Impulses

The "dynamic" and "quasi-static" components I_{dyn} and I_{stat} of the force impulse have been determined separately. These are defined in Fig. 9 where the point M of maximum wave run-up is also shown. By assuming the conservation of momentum, the force impulse $I_w = I_{dyn} + I_{stat}$ should be equal to the momentum of the wave with a mass $m_w = \rho \cdot V_s$ impinging on a wall with a horizontal velocity u_s. The momentum of the wave was also

$$I_w = I_{dyn} + I_{stat}$$
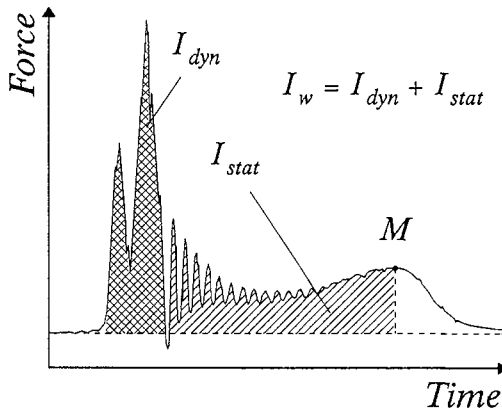
Fig. 9. Force-Impulse Definition Sketch

calculated by using Eqs. (1) and (2) and compared to the force impulse I_w in Fig. 10. It is seen that despite the large scatter, the solitary wave theory still represents a good mean for the approximate evaluation of the loading of vertical structures induced by breaking waves. In average, the wave momentum was slightly larger (7 %) than the force impulse I_w (correlation coeff. = 0.83).
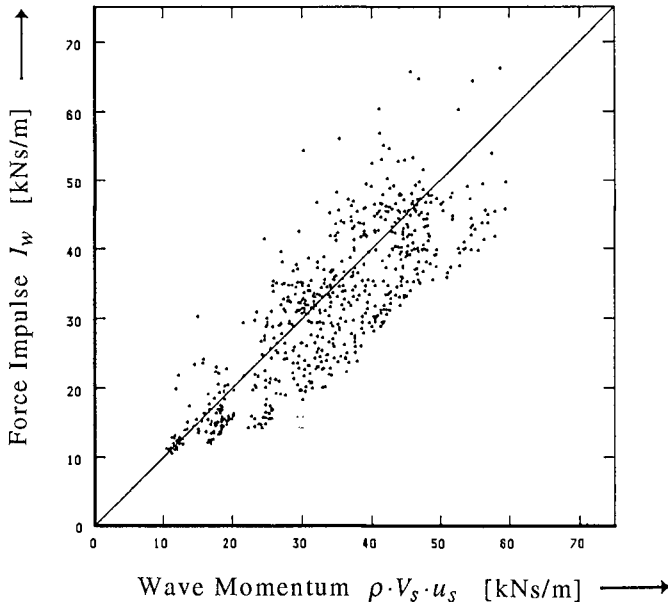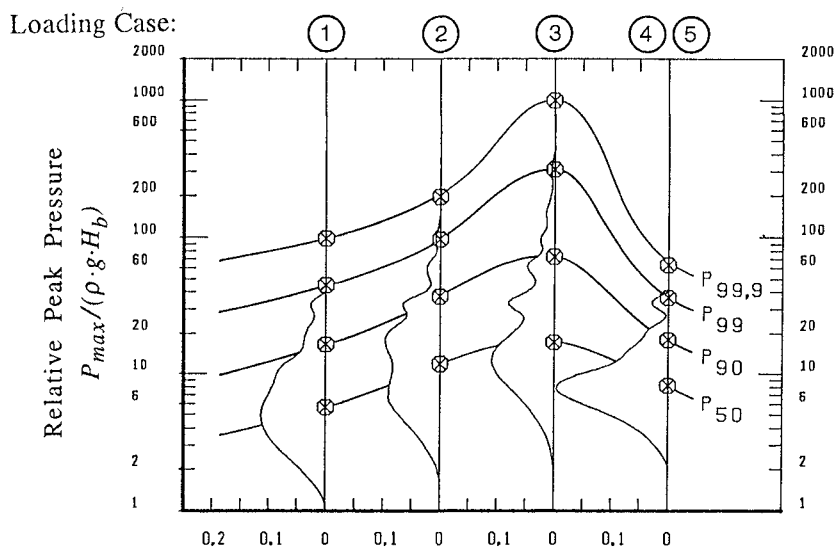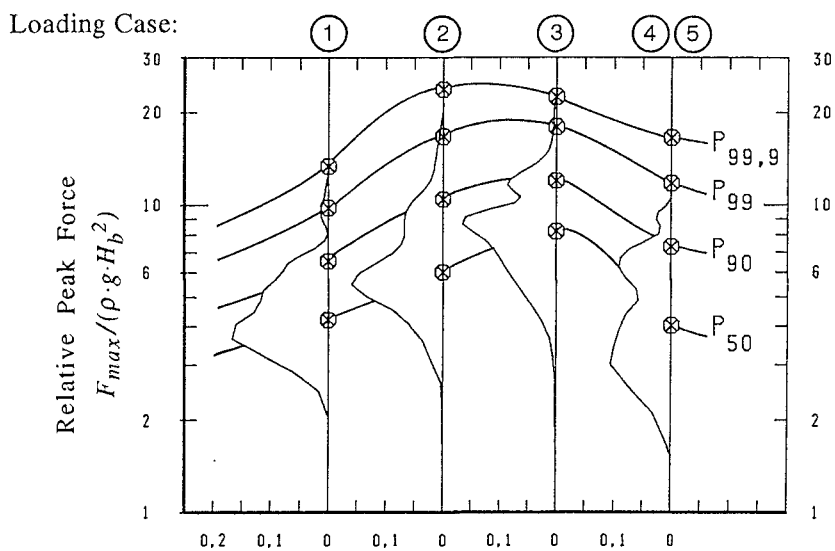

Fig. 10. Force Impulse vs. Wave Momentum

Statistical Analysis of Impact Pressures and Forces

A statistical analysis of the impact pressures and forces recorded for the different loading cases defined in Fig. 2 has been performed for almost 1000 breaking wave impacts. Although this analysis still proceeds, some of the first results may already be discussed below.

Loading Case:

Relative Peak Pressure $P_{max}/(\rho \cdot g \cdot H_b)$

a) Impact Pressures: Relative Frequency of Occurrence (36 Classes)

Loading Case:

Relative Peak Force $F_{max}/(\rho \cdot g \cdot H_b^2)$

b) Impact Forces: Relative Frequency of Occurrence (30 Classes)

Fig. 11.   Statistical Distribution of Impact Pressures and Forces for the
           Different Loading Cases of the Plunging Breaker (see Fig. 2)

a) Peak Pressure $P_{max}/(\rho \cdot g \cdot H_b)$

$$\frac{P_{max}}{\rho \cdot g \cdot H_b} = e^{\frac{(-ln(1-P_u))^{1/c} - a}{b}}$$

$a = -0.282$
$b = +0.499$
$c = 2.2$

LOG - RAYLEIGH
Exponent = 2.2
Corr. Coeff. = 0.9986

b) Peak Force $F_{max}/(\rho \cdot g \cdot H_b^2)$

$$\frac{F_{max}}{\rho \cdot g \cdot H_b^2} = e^{\frac{(-ln(1-P_u))^{1/c} - a}{b}}$$

$a = -0.371$
$b = +0.737$
$c = 2.9$

LOG - RAYLEIGH
Exponent = 2.9
Corr. Coeff. = 0.9988

c) Force Impulse $I_w/(\rho \cdot g \cdot H_b^2)$ [s]

$$\frac{I_w}{\rho \cdot g \cdot H_b^2} = e^{-\left[\frac{ln(-ln(P_u)) + a}{b}\right]}$$

$a = +2.75$
$b = +1.75$

LOG - GUMBEL
Corr. Coeff. = 0.9697
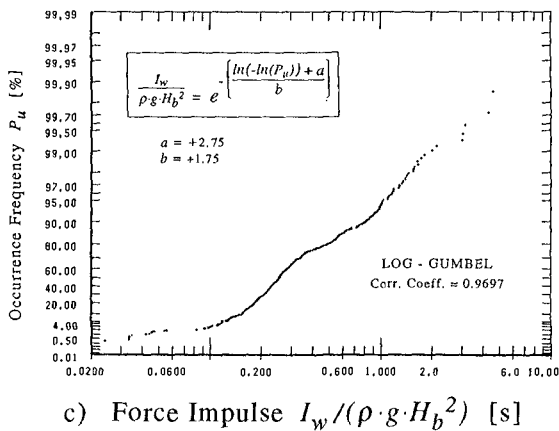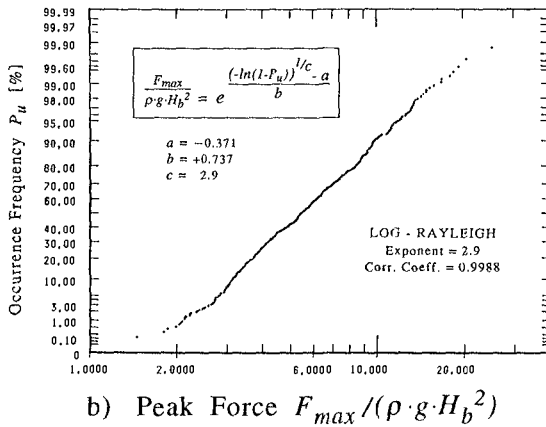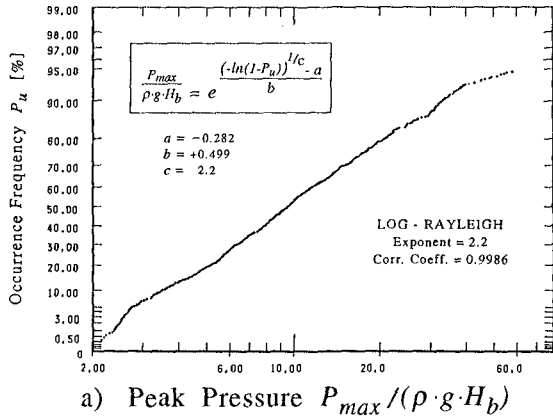
Fig. 12. Statistical Distribution of Impact Loads (n=717 Breaking Waves)

In Fig. 11 the frequency of occurrence of the dimensionless peak pressures and forces is plotted for the different loading cases of the plunging breaker shown in Fig. 2. It is clearly seen that the highest impact pressures occur for loading case 3. On the other hand, the differences between the loading cases are more pronounced for the distribution of impact pressures (Fig. 11a) than for that of the impact forces (Fig. 11b). Further results have also shown that the maximum impact pressures, forces and overturning moments are best described by a LOG-RAYLEIGH distribution whereas the corresponding impulses follow a LOG-GUMBEL distribution (Fig. 12).

Air Content

The air content of the air-water mixture and the air dynamics involved in the impact process represent a further important factor in the generation mechanisms of impact pressures. However, the entrained air could not be directly measured in the model tests. Nevertheless, an attempt is made to use the detailed impact pressures measured at 28 different elevations along the wall for the approximate statistical evaluation of the air content involved in the impact process. This has been done through the sound velocity c_w in the air-water mixture which is evaluated by following the propagation (downward the wall) of a perturbation in the impact pressure traces and distributions (Fig. 5). The identification of the same perturbation at different pressure cells and the phase shifts have been determined from the detailed pressure histories (sampled at 11 kHz) of the pressure gauges under still water level by using FFT-techniques (SCHMIDT, 1993).

Fig. 13. Statistical Distribution of Sound Velocities in Air-Water Mixture during Impact

The results obtained by using this procedure for 201 breaking waves impacting directly on the wall are given in Fig. 13 showing the statistical distribution of the investigated sound velocity c_w, i.e. c_w values between 100 m/s and 450 m/s with an average value of $\overline{c}_w = 212$ m/s occur,

corresponding to air contents $æ = 0.04 - 1.0$ % ($\bar{æ} = 0.2$ %). These velocities actually correspond to speeds at which a perturbation propagates downwards within the air-water mixture. Detailed shock pressure measurements performed by HATTORI and ARAMI (1992) have also shown that this propagation essentially develops within the air-water mixture.

Concluding Remarks

Despite more than 80 years of research work on impact loading of vertical structures subject to breaking waves there are still two basic attitudes related to the design of such structures.

The first attitude consists in simply assuming that impact pressures are not important and thus should not be adopted in the design. The inadequacy of this approach has been demonstrated by the results of the more recent investigations (OUMERACI et.al., 1992; TAKAHASHI et.al., 1992).

The second attitude is to skip the problem of evaluating the design impact load by assuming that the structure can be designed in such a way that impact pressure will not occur. The existing standard design pressure formulae implicitely reflect this attitude. However, it is not advisable to design vertical breakwaters only by applying such formulae, since most of vertical structures will certainly be subject to all conditions of breaking waves during their lifetime.

In fact, the worst loading case for a vertical structure and its foundation is induced by a well-developped plunging breaker. In this respect, the results to be presented in this paper intend to help in assessing the worst impact loads to be considered in a dynamic analysis of the structure and its foundation.

Acknowledgements

References

C.E.R.C. : Shore Protection Manual. Vol. 1, 1984

GALVIN, C. : Breaker type classification on three laboratory beaches. Journal of Geophysical Research, Vol. 73, No. 12, 1966, pp. 3651-3659

GODA, Y. :   Wave forces on a vertical cylinder: Experiments and a proposed method of wave force computation.   Report of the Port and Harbour Technical Research Inst., No. 8, 1964

GODA, Y. :   Random seas and design of maritime structures.   University of Tokio Press, 1985

HATTORI, M. ; ARAMI, A. :   Impact breaking wave pressures on vertical walls.   ASCE, Proc. 23rd ICCE, Venice, 1992 (these proceedings)

MURAKI, Y. :   Field investigations on the oscillations of breakwaters caused by wave action.   Coastal Engineering in Japan, Vol. 9, 1966

OUMERACI, H.; PARTENSCKY, H.-W.; TAUTENHAIN, E.; NICKELS, H. : Large-scale model investigations: a contribution to the revival of vertical breakwaters.   Inst. Civil Engineers, Proc. Conf. Coastal Structures & Breakwaters, London, 1991

OUMERACI, H. ; PARTENSCKY, H.-W. ; TAUTENHAIN, E. :   Breaking wave loads on vertical gravity structures.   Proc. 2nd Int. Conf. Offshore & Polar Eng., ISOPE'92, Vol. 3, San. Francisco, 1992, pp. 532-539

OUMERACI, H. ; KLAMMER, P. ; PARTENSCKY, H.-W. : Classification of breaking wave loads on vertical structures.   ASCE, Journal of the Waterways, Port, Coastal and Ocean Eng. (paper accepted), 1993

SCHMIDT, R. :   Druckschlagbelastung senkrechter Wellenschutzbauwerke. Ph.D-Thesis, University of Hannover, 1993 (in German)

TAKAHASHI, S. ; TANIMOTO, K. ; SHIMOSAKO, K. :   Experimental study on impulsive pressures on composite breakwaters.   Report of the Port and Harbour Tech. Research Inst., Vol. 31, No. 5, 1992

WEGGEL, J. R. :   The impact pressures of breaking water waves. Ph.D-Thesis, University of Illinois, 1968